# Study of Grain Boundary Motion in Ice Bicrystals†

**C. L. Di Prinzio* and O. B. Nasello**

*Facultad de Matemática Astronomía y Física, Universidad Nacional de Córdoba, Ciudad Universitaria, 5000 Córdoba, Argentina*

*Received: October 11, 1996; In Final Form: July 25, 1997*⊗

The motion of $\langle 10\bar{1}0\rangle/\theta$ ice grain boundaries is studied using the "Sun−Bauer" technique. The samples were annealed at temperatures between −2 °C and −20 °C, for times up to 1400 h, and $M\gamma$ values for mixed and tilt boundaries were determined ($M$ and $\gamma$ are the mobility and the excess of free energy per unit area of the grain boundary, respectively). For each rotation angle $\theta$ and annealing temperature, a large scattering is found in $M\gamma$ values. This scattering is related to the dependence of migration on grain boundary inclination. The obtained results are specially analyzed taking into account CSL concepts and grain boundary migration in anisotropic materials.

## 1. Introduction

The motion of grain boundaries in ice has been widely investigated in an attempt to identify relationships between the structure of the analyzed samples and the conditions to which these were submitted from their formation up to their analysis. These studies have been generally performed studying grain growth in polycrystalline samples. However, those carried out in bicrystalline samples are a powerful tool to understand the structure and properties of grain boundaries.

Grain boundary (GB) migration rates in bicrystalline ice samples were first investigated by Hondoh and Higashi (1979)[1] (HH). These authors studied in detail the migration of $\langle 10\bar{1}0\rangle$/34° tilt boundaries following the Sun−Bauer technique (Sun and Bauer, 1970[2]). A remarkable anisotropy of the migration rate was found. GBs with the rotation axis, $\omega$, parallel to the direction of the GB velocity ($\omega_{||}$) exhibited values of the product $M\gamma$ ($M$ and $\gamma$ are the mobility and the excess of free energy per unit area of the grain boundary, respectively) higher than those with normal $\omega$ ($\omega_{\perp}$). Furthermore, it was found that GBs with low values of $M\gamma$ displayed facets whose planes coincide with high density planes of the coincidence site lattice (CSL).

Nasello et al. (1992)[3] studied GB migration in bicrystalline samples obtained from rotations around the $\boldsymbol{a} = \langle 10\bar{1}0\rangle$, $\boldsymbol{b} = \langle 11\bar{2}0\rangle$, and $\boldsymbol{c} = \langle 0001\rangle$ axes. The Sun−Bauer technique was also applied. For $\boldsymbol{b}$ and $\boldsymbol{c}$ rotation axes, which have associated CSLs with high density planes, low values of $M\gamma$ were found, in concordance with HH. For the $\boldsymbol{a}$ axes, only two rotation angles $\theta$ were studied, $\theta = 35°$ and $\theta = 45°$. In these cases, a nondefinite relationship between the $M\gamma$ values and the associated CSL was found. Due to the relevance of extending this type of research to a larger number of ice GBs obtained from rotations around the $\langle 10\bar{1}0\rangle$ axis, new experiments of grain boundary migration have been carried out, using the Sun−Bauer technique. The obtained results have been specially analyzed taking into account the results described by HH and the theoretical treatment developed by Di Prinzio et al. (1995)[4] for GB migration in anisotropic materials.

## 2. Experimental Methods

The samples were grown following the same procedure described by Nasello et al. (1992). Namely, the ice bicrystals were obtained using a cell, 10 × 10 × 5 cm in size, which contains two brass rods screwed to its bottom. To obtain the bicrystals, the brass rods were placed in contact with a lead block inside a freezer at a temperature of about −27 °C. Monocrystalline ice seeds of about 0.5 cm per side were attached to the inner ends of the brass rod, and the cell was filled with purified water (conductivity less than 0.6 $\mu$S). The $\boldsymbol{c}$ axes of both seeds lay on a plane parallel to the surface of the cell bottom and formed an angle $\theta$ .The walls of the cell were heated so that the heat of freezing could flow only throughout the brass rod. In this way, after 24 h, $\langle 10\bar{1}0\rangle/\theta$ bicrystals of about 5 × 5 × 1.5 cm in size were obtained. From the developed specimens, slices of approximately 4 cm thickness were sawed with their long sides parallel to the GB. The samples to be annealed, 1 × 1 × 0.5 cm in size, were cut from such slices, according to the $\omega_{||}$ and the $\omega_{\perp}$ configurations, and the sample surfaces were polished with a microtome. The bicrystal orientations were determined by using formvar replicas. Rotation angles of $\theta = 15°$, 20°, 35°, 45°, 60°, and 90° were prepared according to the $\omega_{||}$ configuration and of $\theta = 20°$, 45°, 60°, and 90° according to the $\omega_{\perp}$ one. The samples were introduced in a transparent acrylic box filled with silicone oil sealed to avoid ice evaporation and placed inside boxes at constant temperatures of $T = -2$, −6, −10, and −20 °C for times up to 1440 h. The grain boundary migration was registered, at different times $t$, photographing the samples viewed in an optical microscope between crossed polaroids. From the photographs the distances "$a$" traveled by the boundary (see Figure 1) were measured, and for each sample one $M\gamma$ value was obtained using the expression

$$a^2 = M\gamma f(\alpha)t \qquad (1)$$

with the magnification factor $f(\alpha)$ given as a function of α by ref 2.

## 3. Results

The values of $M\gamma$ found for $\langle 10\bar{1}0\rangle/\theta$ GBs in the $\omega_{\perp}$ configuration at $T \leq -10$ °C are given in Table 1. In order to show both the scattering of the results and their mean tendencies as a function of $\theta$, we have represented, in adjacent columns of Table 1 the $M\gamma$ values obtained from single experiments and their averages $\overline{M\gamma}$. In this table, a large scattering in the $M\gamma$ values corresponding to different $\theta$ values may be observed. Generally, the experimental uncertainty for each $M\gamma$ value was

† This paper was originally submitted to appear in the Ice Symposium issue of *J. Phys. Chem. B* [**1997**, *101*, 6079−6312].

⊗ Abstract published in *Advance ACS Abstracts,* September 1, 1997.

S1089-5647(96)03258-0 CCC: $14.00 

**TABLE 1: Values of $M\gamma$, Expressed in $10^{-8}$ cm$^2$ s$^{-1}$, Corresponding to $\langle 10\bar{1}0\rangle/\theta$ $\omega_\perp$ Grain Boundaries Annealed at Different Temperatures $T$**

| | $T$ | | | | | | | | | | | |
|---|---|---|---|---|---|---|---|---|---|---|---|---|
| | −2 °C | | | | | −6 °C | | | | −10 °C | | | |
| $\theta$ | $M\gamma$ | | | | $\overline{M\gamma}$ | $M\gamma$ | | | $\overline{M\gamma}$ | $M\gamma$ | | | $\overline{M\gamma}$ |
| 15° | 0.3 | | | | 0.3 | 0.06 | | | 0.06 | 0.02 | | | 0.02 |
| 20° | 0.5 | | | | 0.5 | 0.09 | | | 0.09 | * | * | | * |
| 35° | 1.1 | 1.1 | 0.5 | 0.3 | 0.8 | 0.09 | | | 0.09 | 0.07 | | | 0.07 |
| 45° | 6.0 | 1.1 | 1.0 | | 2.7 | 0.8 | 0.2 | 0.4 | 0.5 | 0.08 | 0.05 | 0.04 | 0.06 |
| 60° | 2.2 | 1.4 | 0.8 | | 1.5 | 1.5 | | | 1.5 | * | * | | * |
| 90° | 1.2 | 0.3 | | | 0.8 | 0.8 | 0.07 | | 0.4 | * | * | * | * |

[a] * = no measurable boundary migration.

**TABLE 2: Values of $M\gamma$, Expressed in $10^{-8}$ cm$^2$ s$^{-1}$, Corresponding to Pairs of $\langle 10\bar{1}0\rangle/\theta$ $\omega_\perp$ and $\omega_\parallel$ Grain Boundaries Annealed at Different Temperatures $T$**

| | $\theta$ | | | | | | | |
|---|---|---|---|---|---|---|---|---|
| | 20° | | 45° | | 60° | | 90° | |
| $T$ | $\omega_\perp$ | $\omega_\parallel$ | $\omega_\perp$ | $\omega_\parallel$ | $\omega_\perp$ | $\omega_\parallel$ | $\omega_\perp$ | $\omega_\parallel$ |
| −2 °C | 0.5 | 0.8 | 6.0 | 0.4 | 2.2 | 6.0 | 1.2 | 3.2 |
| −6 °C | 0.09 | 0.4 | 0.8 | 0.1 | 1.5 | 4.0 | 0.8 | 3.0 |

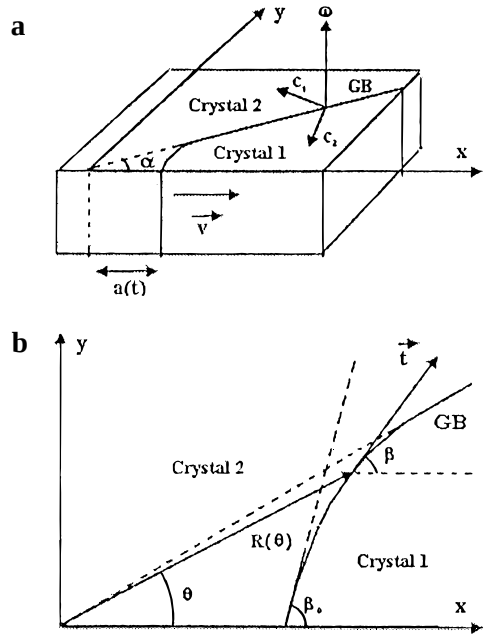


**Figure 1.** Schematic representation of the ice bicrystals studied.

lower than 30%, so this scattering is certainly not a simple consequence of an experimental error. Taking into account that the samples were not prepared so as to have the same inclination of their moving GBs, the observed scattering may be a consequence of the dependence of the GB migration on the GB inclination. At $T = -20$ °C only for the $\langle 10\bar{1}0\rangle/45°$ GB in the $\omega_\perp$ configuration was a measurable $M\gamma$ value obtained ($M\gamma = 0.02 \times 10^{-8}$ cm$^2$ s$^{-1}$).

In Table 1 it is also interesting to note that, as in other materials (see for instance Demianczuck and Aust (1972)[5] and Gottstein and Schwarzwer (1992)[6]), the mean values of $M\gamma$ corresponding to each temperature have a tendency to increase with $\theta$, up to a maximum attained for $\theta$ values between 45° and 60°. On the other hand, for each $\theta$, it can be observed that the $\overline{M\gamma}$ values decrease with the annealing temperature. This behavior is typical, since GB migration rates usually display characteristics of a thermally activated phenomenon. For each $\theta$, activation energy values were estimated, finding that they are within the range 0.6−4 eV. These values agree with those observed by other authors (Ceppi (1985),[7] Azuma and Higashi (1978)[8]). However, due to the large scattering observed in the values of $M\gamma$ corresponding to certain values of $\theta$, these values of activation energy may be meaningless.

The $M\gamma$ values corresponding to pairs of specimens prepared from the same bicrystal, in the $\omega_\perp$ and $\omega_\parallel$ configurations, are presented in Table 2. This table shows that in all the studied cases there is a marked difference between the $M\gamma$ values corresponding to each type of specimen. For the rotation angles $\theta = 20°$, 60°, and 90° the $M\gamma$ values corresponding to $\omega_\parallel$ are 1.6−4.4 times higher than those corresponding to $\omega_\perp$. This behavior is similar to that reported by HH. Only for the rotation angle $\theta = 45°$ was the opposite observed. It is interesting to notice that only in this case did the extremity of the moving $\omega_\parallel$ boundary show a faceted structure.

## 4. Discussion and Conclusions

In the present work, results were analyzed on the basis of the CSL concept also used by HH. This analysis was carried out using the CSL corresponding to the different values of $\theta$ obtained by Gonzalez et al. (1996).[9]

The CSLs found by González et al. were obtained using an ice crystalline structure with an axis ratio given by $c^2/a^2 = 8/3$, which is quite close, though not identical, to experimental values measured on ice.

Comparing the $\langle 10\bar{1}0\rangle/\theta$ bicrystalline samples studied in the present work with the CSLs reported by González et al. (1996), it was observed that none of the former have an associated CSL with $\Sigma < 50$. However, as noted by King and Singh (1994),[10] in noncubic materials, where exact CSLs are relatively rare, real GB deviations from an exact CSL grain boundary, both in misorientation and axial ratios, may be explained by an array of grain boundary dislocations in the corresponding displacement shift complete (DSC) lattice. In these cases, it is possible that an apparently arbitrary misorientation be represented by a well-spaced dislocation array corresponding to a CSL that is very far away, in both misorientaion and axial ratios, from the experimental values. So, in order to find out a correlation of GB special properties with CSL structures, it is essential to have a complete list of candidate CSLs with different axial ratios and to study, in all of them, the array of dislocations needed to reproduce the grain boundary of interest, which is quite a difficult task, as pointed out by the authors themselves. Notwithstanding, as these authors also cited, some GB properties

**TABLE 3: Values for the Studied ⟨10$\bar{1}$0⟩/$\theta$ Boundaries of Σ (Volume Density of Coincidence Sites), 1/Γ (Γ Planar Density of Coincidence Site of the CSL High-Density Plane), and Miller Indices of the Crystal Planes Belonging to Each Side of the GB, Which Are Parallel to a High-Density Plane of the Corresponding CSL. 1/Γ Is Expressed in Units of the Ice Lattice Parameter in the *a* Direction. 01, 02, 03, and 12 Represent the Planes, Parallel to the Rotation Axis $\omega$, with the Highest Density Γ**

| | | 01 | | 02 | | 03 | | *12* | |
|---|---|---|---|---|---|---|---|---|---|
| $\theta$ | Σ | *1/Γ* | *indices* | *1/Γ* | *indices* | *1/Γ* | *indices* | *1/Γ* | *indices* |
| 23.1° | 25 | 6.9 | {6331}<br>{6331} | 13.9 | {10558}<br>{10558} | 16.8 | {4137}<br>{2119} | 16.8 | {2119}<br>{4137} |
| 34.0° | 35 | 5.8 | {2111}<br>{2111} | 15 | {30151516}<br>{30151516} | 30.3 | {105517}<br>{2116} | 30.3 | {2116}<br>{105517} |
| 44.4° | 14 | 9.1 | {2116}<br>{2111} | 7.4 | {2111}<br>{2116} | 10.3 | {2118}<br>{2118} | 10.3 | {6334}<br>{6334} |
| 62.2° | 11 | 3.3 | {2112}<br>{2112} | 8.0 | {63316}<br>{63316} | 16.8 | {2119}<br>{4227} | 16.8 | {4227}<br>{2119} |
| 88.8° | 49 | 10.3 | {6339}<br>{6339} | 19.7 | {105516}<br>{105516} | 23.4 | {8443}<br>{20101013} | 23.4 | {20101013}<br>{8443} |

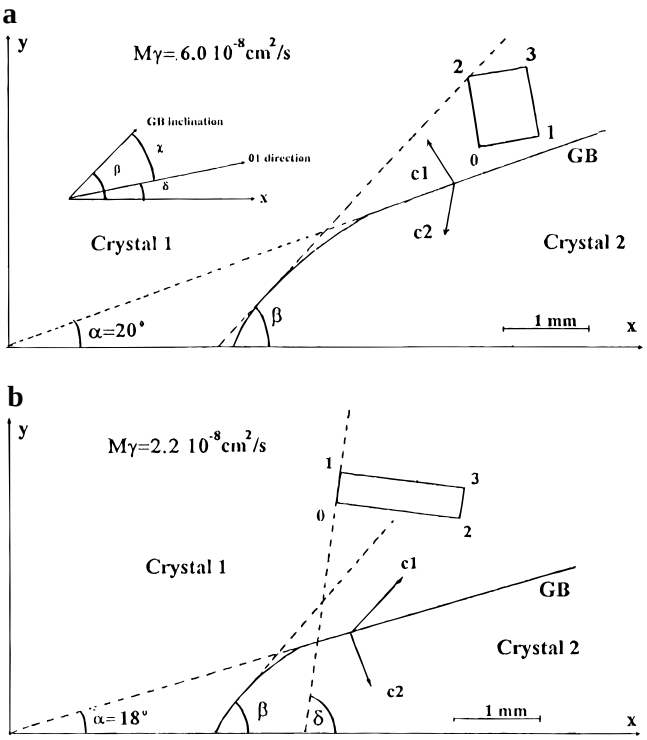


**Figure 2.** GB inclination relative to the corresponding CLS unit cell: (a) $\omega_{\perp}$⟨10$\bar{1}$0⟩/45° and (b) $\omega_{\perp}$⟨10$\bar{1}$0⟩/60° $T = -2$ °C. The numbers located at the unit cell correspond to the planes presented in Table 3.

found in noncubic materials have been satisfactorily accounted for using exact CSLs with axial ratios similar to those given by experimental values. On the other hand, HH has explained certain characteristics of GB migration rate on ice in a satisfactory manner using an exact CSL and the geometric criteria always used for cubic materials. Regarding ice crystals, there are no detailed GB studies employing these concepts. Moreover, little is known about the structure and properties of grain boundaries. For this reason we found that it would be useful to analyze the experimental results using the CSLs closest to the considered GB.

Thus, the studied ⟨10$\bar{1}$0⟩/20°, 35°, 45°, 60°, and 90° GBs were analyzed using the ⟨10$\bar{1}$0⟩/23.1°, 34°, 44.4°, 62.2°, and 88.8° CLSs, which are the closest CSLs with $\Sigma < 50$ obtained by González et al. (1996).

Table 3 shows, for each studied ⟨10$\bar{1}$0⟩/$\theta$ boundary, the associated values of Σ, 1/Γ, and Miller indices of the CSL high-density planes. Comparing the $M\gamma$ values presented in Table 1 with the CSL's characteristics shown in Table 3, it is not possible to find, for all the studied samples, a correlation between them. For instance, as Table 3 shows, the ⟨10$\bar{1}$0⟩/44.4° and ⟨10$\bar{1}$0⟩/62.2° CSL GBs have lower values of Σ, 1/Γ, and Miller indices than the others. According to the geometric criteria for low interfacial energy (Sutton and Balluffi, 1987[11]), these orientations could have lower values of the GB energy and, as shown in previous works,[3] they could have lower values of the migration rate. However, looking at Table 1, it can be observed that the $M\gamma$ values corresponding to the associated GBs ⟨10$\bar{1}$0⟩/45° and ⟨10$\bar{1}$0⟩/60° are higher than the others.

In Figure 2a,b the orientation of the GBs relative to the corresponding CSL unit cell are shown, respectively, for the $\omega_{\perp}$⟨10$\bar{1}$0⟩/45° and $\omega_{\perp}$⟨10$\bar{1}$0⟩/60° cases annealed at $T = -2$ °C. In this figure the stationary shapes of the GBs are shown together with the corresponding CSL unit cell projected onto the plane of the figure (the numbers located at the unit cell correspond to the planes presented in Table 3). This figure shows that a section of the moving boundary runs throughout planes parallel to the 03 high-density plane of the CSL in the ⟨10$\bar{1}$0⟩/45° case, but in the ⟨10$\bar{1}$0⟩/60° case the GB never runs parallel to the 01 or 02 high-density planes. According to HH the $M\gamma$ values corresponding to the first sample should be lower than those of the second one; however, the opposite was found. Thus, it could be concluded that the results obtained in the present work are not well interpreted using the CSL.

It may be noted that in the preceding analysis the $M\gamma$ values were obtained using eq 1, which was developed for nonanisotropic materials. However, as shown in a previous work,[4] for anisotropic materials this equation changes. In fact, when the GB migration is studied in anisotropic materials following the Sun−Bauer technique, it is found that instead of eq 1 the following expressions must be used:

$$a^2 = 2\overline{M\gamma}_{\text{eff}} F_{\gamma}(\alpha) t \qquad (2)$$

where

$$\overline{M\gamma}_{\text{eff}} = \frac{\int_{\beta_0}^{\alpha} M\gamma_{\text{eff}} \mathrm{d}\beta}{(\beta_0 - \alpha)} = \frac{\int_{\beta_0}^{\alpha} M\left(\gamma + \frac{\partial^2\gamma}{\partial\beta^2}\right) \mathrm{d}\beta}{(\beta_0 - \alpha)}$$

and

$$F_{\gamma}(\alpha) = (\beta_0 - \alpha)\frac{R^2(0)}{\int_0^{\alpha} R^2(\theta)\, \mathrm{d}\theta}$$

As shown in Figure 1b, $R(\theta)$ is the parametric representation of the GB stationary form, $\theta$ is the polar angle measured from the $x$ axis, $\beta$ is the angle between the tangent $\boldsymbol{t}$ to the GB at the point $(R(\theta),\theta)$ and the $x$ axis ($\beta$ is a measurement of the GB inclination), and $\alpha$ and $\beta_0$ are equal to the $\beta$ angles corresponding to the asymptotic and initial part of the GB, respectively .

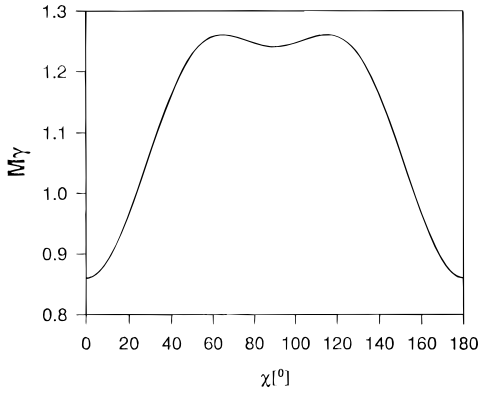


**Figure 3.** $M\gamma(\chi)$ function chosen to represent the $\omega_{\perp}\langle 10\bar{1}0\rangle/60°$ GB.

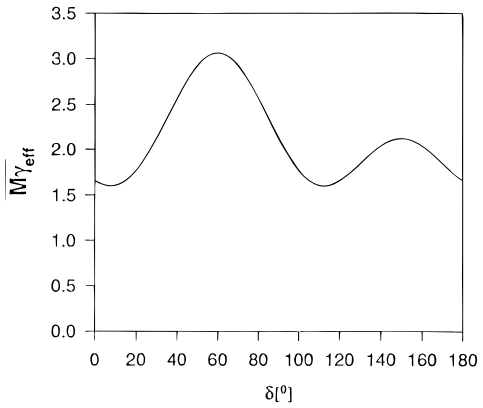


**Figure 4.** $\overline{M\gamma_{eff}}$ vs $\delta$ obtained from eq 2 with $M\gamma(\chi)$ shown in Figure 3 with $\beta = \delta + \chi$.

As noted in ref 4, if the shape of the studied GB is not very different from that obtained following Mullins' (1957)[12] calculations with $\gamma = \text{const}$, it results that $F_{\gamma}(\alpha) \cong f(\alpha)$. In the samples studied in the present work this condition was generally fulfilled. Thus, due to the similarities existing between eq 1 and eq 2, the values of $\overline{M\gamma}$ reported in Tables 1 and 2 can be reinterpreted as values of $\overline{M\gamma_{eff}}$. To analyze these values, it must be born in mind that they are the mean values of $M(\gamma + (\partial^2\gamma/\partial\beta^2)$ along the moving boundary, so they depend not only on the values of $M\gamma$ as a function of $\beta$ but also on the $\alpha$ and $\beta_0$ angles.

Unfortunately, in ice $M\gamma$ is not known as a function of the GB inclination, so we qualitatively analyzed the obtained results proposing a $M\gamma$ function using the CSL concepts. We represented this function by a $M\gamma(\chi)$ function, where $\chi$ is an angle that measures the GB inclination with respect to the direction of the CSL high-density plane (see Figure 2). Following the geometric criteria for low interfacial energy, the GBs with lower energy could be those with lower $1/\Gamma$ values and lower Miller indices of the crystallographic planes belonging to each crystal. Thus, assuming $M = \text{const}$, the results presented in Table 3 indicate that, for instance, the $M\gamma(\chi)$ function for the $\omega_{\perp}\langle 10\bar{1}0\rangle/60°$ boundaries might have a period $\pi$ and two local minima at $\chi = 0$ and $\pi/2$, corresponding to the planes named 01 and 02 in Table 3, respectively. The minimum associated with the plane 01 could have a lower energy value than that corresponding to the 02 plane. A possible function with these characteristics is shown in Figure 3. To analyze the experimental results, $\overline{M\gamma_{eff}}$ values must be evaluated using eq 2. To perform this calculation, it must be noted that from Figure 2 it is inferred that it is $\beta = \delta + \chi$, where $\delta$ is the angle between the highest density plane of the CSL in the studied sample and the $x$ axis.

Figure 4 shows the value of $\overline{M\gamma_{eff}}$ as a function of $\delta$ obtained from the function shown in Figure 3 for $\alpha$ and $\beta_0$ angles equal to 30° and 90°, respectively, which are similar to those used in the present experimental design. In Figure 4 it can be seen that the $\overline{M\gamma_{eff}}$ values vary within a range that approximately coincides with that of $M\gamma$ reported in Table 1, for $\theta = 60°$ and $T = -2$ °C. This result indicates that using $M\gamma(\chi)$ functions as those shown in Figure 3, the observed scattering in the $M\gamma$ values reported in Table 1 could be explained. On the other hand, in Figure 4 it may be noted that $\overline{M\gamma_{eff}}$ ($\delta$) has local minima at $\delta = 10°$ and $\delta = 110°$ and a maximum at $\delta = 60°$. Taking into account that $\delta$ is the angle between the CSL highest density plane and the $x$ axis, it can be inferred that when the GB runs over the high-density planes of the CSL, the corresponding $\overline{M\gamma_{eff}}$ values, and consequently the migration rates, are the highest. Consequently this result could explain why the migration rate corresponding to the case shown in Figure 2a is higher than that of Figure 2b. Similar studies have been performed for the other orientations, and in general, a qualitative agreement between the experimental and theoretical results was found. Thus, the present results show that with a $M\gamma(\chi)$ function like that shown in Figure 3, the $\overline{M\gamma_{eff}}$ values experimentally obtained can be qualitatively reproduced.

Since the function shown in Figure 3 was built adopting the geometric criteria of the CSL theory, it may be concluded that this theory satisfactorily explains the GB migration in ice bicrystals provided that the GB equation of motion corresponding to anisotropic materials is also considered. To quantitatively check this assertion, it must be noted, however, that the $M\gamma(\chi)$ function corresponding to each GB misorientation should be determined.

## References and Notes

(1) Hondoh, T.; Higashi A. *Phil. Mag. A* **1979**, *31*, 138.
(2) Sun, R. C.; Bauer, C. L. *Acta Metall.* **1970**, *6*, 635.
(3) Nasello, O. B.; Di Prinzio, C. L.; Levi, L. *Physics and Chemistry of Ice*; Hokkaido University Press: Sapporo, 1992; p 206.
(4) Di Prinzio, C. L.; González K, B.; Nasello, O. B. *Acta Metall.* **1995**, *43*, 6.
(5) Demianczuck, D. W.; Aust, K. T. *Acta Metall.* **1972**, *23*, 1149.
(6) Gottstein, G.; Schwarzwer, F. *Mater. Sci. Forum* **1992**, *94*−*95*, 187.
(7) Ceppi, E. A. Doctoral Thesis, Facultad de Matemática Astronomía y Física, Universidad Nacional de Córdoba, 1985.
(8) Azuma, N.; Higashi, A. *J. Phys. Chem.* **1978**, *87*, 4139.
(9) González K, B.; Di Prinzio, C. L.; Nasello, O. B. *J. Phys. Chem. B* **1997**, *101*, 6243.
(10) King, A. H.; Singh, A. *J. Phys. Chem. Solids* **1994**, *55*, 1023.
(11) Sutton, P.; Balluffi, R. W. *Acta Metall.* **1987**, *35*, 2177.
(12) Mullins, W. W. *J. Appl. Phys.* **1957**, *59*, 1341.
(13) This research was supported by CONICET, CONICOR, and Fundación Antorchas.